Analysis of Conformational Changes in Bacteriorhodopsin Upon Retinal Removal

Josep Cladera, Jaume Torres, and Esteve Padrós
Unitat de Biofísica, Departament de Bioquímica i de Biologia Molecular, Facultat de Medicina, Universitat Autònoma de Barcelona, 08193 Bellaterra, Barcelona, Spain

ABSTRACT The conformation of bacterioopsin in the apomembrane has been studied by Fourier transform infrared spectroscopy. Resolution enhancement techniques and curve-fitting procedures have been used to determine the secondary structural components from the amide I region. Bacterioopsin contains about 54% helicoidal structure (α_I and α_{II} helices + 3_{10} turns), 21% sheets, 16% reverse turns, and 9% unordered structure. Thus, after retinal removal, all of the secondary structural types of bacteriorhodopsin remain present, and only slight quantitative differences appear. On the other hand, H/D exchange studies show that there is a higher degree of exchange for reverse turns and protonated carboxylic lateral chains in bacterioopsin as compared to bacteriorhodopsin. This gives further support to the idea of a more open tertiary structure of bacterioopsin, and to the consideration of the retinal molecule as an important element in complementing the interhelical interactions in bacteriorhodopsin folding.

INTRODUCTION

Bacteriorhodopsin (BR), the unique protein present in the purple membrane of *Halobacterium salinarium*, transports protons from the interior to the exterior of the cell, thus creating an electrochemical gradient (Oesterhelt and Stoeckenius, 1973; for recent reviews see Khorana, 1988; Henderson et al., 1990; Ebrey, 1993; Lanyi, 1993). The driving force for this transport is provided by light, which is collected by a retinal molecule bound to the protein by a protonated Schiff base. The retinal molecule constitutes the central element of BR function (Rothschild, 1992). Besides acting as an antenna to capture photon energy and to transmit this energy to the protein moiety, retinal also influences the structure of BR. After bleaching, the membrane does not show the characteristic paracrystalline arrangement of the protein in the lipid bilayer (Stoeckenius and Bogomolni, 1982), and the protein conformation seems to be less compact than that of bacteriorhodopsin (Acuña et al., 1984; Cladera et al., 1992a). Futhermore, bacterioopsin (BO) incorporated into liposomes becomes leaky to protons, whereas BR is impermeant (Burghaus and Dencher, 1989). Other observations refer to the fact that retinal removal affects the properties of the cation-binding sites (Duñach et al., 1986). Despite these changes, Raman (Vogel and Gärtner, 1987) and infrared (IR) studies (Duñach et al., 1989) indicate that the secondary structure of BO is very similar to that of BR. On the other hand, infrared spectra of purple and bleached membranes in D_2O show similar secondary structural changes upon thermal denaturation (Cladera et al., 1992a).

In this work we obtain more detailed information about the BR secondary structural changes induced by retinal removal. Curve-fitting of the deconvoluted infrared spectrum was used, following a general procedure to determine the best deconvolution parameters. This method has recently been used to estimate the secondary structure of BR (Cladera et al., 1992b).

MATERIALS AND METHODS

Sample preparation

Purple membrane was obtained from *Halobacterium salinarium*, strain S9, as described (Oesterhelt and Stoeckenius, 1974). Bleached membrane was obtained by illumination of suspensions of purple membrane (2.5×10^{-5} M BR) with yellow light in the presence of 1 M hydroxylamine and 4 M NaCl at pH 7.5 as described (Oesterhelt et al., 1974). Membrane suspensions in water (pH 6.0) at about 20 mg/ml protein concentration were placed in 6 μm path-length CaF_2 IR cells with tin spacers. Suspensions in D_2O were prepared by washing the membrane three times with D_2O and keeping the final suspension overnight before data collection, to achieve a good D/H exchange. Samples in D_2O (pD 6.0) at a protein concentration of about 20 mg/ml were placed in 25 μm path-length CaF_2 IR cells with teflon spacers.

Infrared data acquisition

IR spectra were acquired on a Mattson Polaris Fourier transform infrared spectrometer equipped with a mercury cadmium telluride detector, working at an instrumental resolution of 1 cm^{-1}. One thousand scans were averaged with a sample shuttle, apodized with a triangle function, and Fourier-transformed. The spectrometer was continuously purged with dry air (dew point lower than $-60°C$). The sample temperature was set at 20°C. To obtain the pure spectra of bleached membrane, spectra of the solvent were collected under identical conditions, and digital subtractions were done with the computer. The criteria for a good subtraction were the removal of the water band near 2130 cm^{-1} and obtaining a flat line between 1800 and 2000 cm^{-1}. This region was also useful for checking the absence of residual water vapor peaks.

Received for publication 1 November 1995 and in final form 19 March 1996.

Address reprint requests to Dr. Esteve Padrós, Unitat de Biofísica, Facultat de Medicina, Universitat Autònoma de Barcelona, 08193 Bellaterra, Barcelona, Spain. Tel.: 34-3-581-1870; Fax: 34-3-581-1907. E-mail: epadros@cc.uab.es.

0006-3495/96/06/2882/06 $2.00

Resolution enhancement and curve-fitting

To obtain the optimum deconvolution parameters (full width at half-height (FWHH) and k), we followed the next steps: 1) Absorption experimental spectra were Fourier self-deconvoluted by using the programs developed by Moffat et al. (1986), with a Lorentzian band shape and several pairs of FWHH and k values. (The resolution enhancement factor (k) used in the deconvolution process is defined as the ratio between the bandwidth values before and after the mathematical treatment (Surewicz and Mantsch, 1988).) From previous essays with different proteins, the initial FWHH and k values were set at 14 cm^{-1} and 2.5, respectively. In all cases the k values were kept below log (signal/noise), as indicated by Mantsch et al. (1988). 2) A least-squares iterative curve-fitting (Spectra Calc v2.21, from Galactic) was performed over each deconvoluted spectrum, using a Gaussian band shape and allowing the peak positions, heights, and bandwidths to vary simultaneously until a good fit was achieved. 3) The bands obtained in 2) were transformed to 100% Lorentzian bandshape, and the bandwidth was multiplied by the k factor. The addition of these bands resulted in what we called a synthetic spectrum, which was compared with the experimental one (see Fig. 2 *B*). The deconvolution parameters FWHH and k, producing a synthetic spectrum more similar in shape to the original experimental one, were taken as the more suitable deconvolution parameters and were used in the quantification.

RESULTS AND DISCUSSION

Fig. 1 shows the original infrared spectra of bleached membrane suspensions in H_2O and in D_2O. One of the principal problems in the analysis of protein secondary structure by infrared methods is the selection of the best deconvolution parameters. Fig. 2 illustrates the process followed in the selection of these parameters as explained in Materials and Methods. Fig. 2 *A* shows deconvoluted spectra of BO in H_2O, obtained by using different values for the parameters FWHH and k. Important differences can be observed for the most relevant bands. For example, the only band that appears near 1660 cm^{-1} in the deconvolution FWHH = 14/k = 2.5 shows a clear shoulder in the deconvolution 13/2.7. In both cases, curve fittings of these spectra were performed, and two synthetic spectra were generated by following the procedure indicated in Materials and Methods. Fig. 2 *B* shows that a closer similarity between synthetic and original experimental spectra was attained using FWHH = 13 and k = 2.7 than with FWHH = 14 and k = 2.5. Other values for these parameters also gave synthetic spectra more dissimilar from the original; thus, we took 13/2.7 as the best deconvolution parameters for this sample. For spectra corresponding to the sample in D_2O, the best values for FWHH and k were found to be 13 cm^{-1} and 2.4, respectively (spectra not shown).

Fig. 3 *A* shows the deconvoluted spectra of BO in H_2O and D_2O. By comparing the spectrum of BO in H_2O with that corresponding to BR (Cladera et al., 1992b) (Fig. 3 *B*), it is clear that the main difference appears for the well-defined maximum at 1658 cm^{-1} in the BR spectrum, which in BO converts to a maximum at 1659 cm^{-1} with a shoulder at 1654 cm^{-1}. To quantify these changes, we performed curve fitting over the deconvoluted spectra, as shown in Fig.

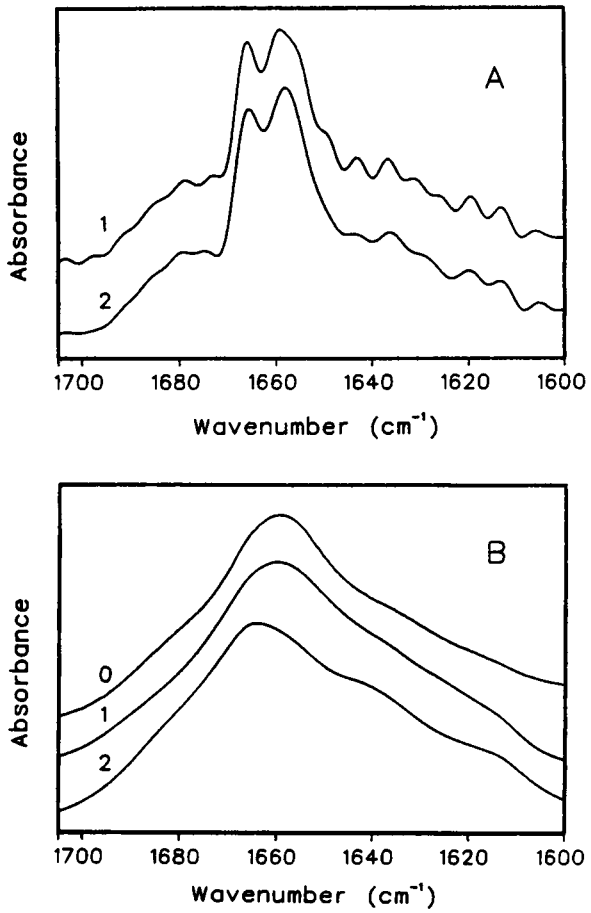

FIGURE 2 Example of the procedure followed to determine the best deconvolution parameters. (*A*) Deconvoluted spectra (amide I region) of bacterioopsin in H_2O obtained with the parameters FWHH = 13, k = 2.7 (1); and FWHH = 14, k = 2.5 (2). (*B*) Original absorption spectrum (0); synthetic spectra generated from the deconvoluted spectra (1) and (2) of *A*, as described in Materials and Methods.

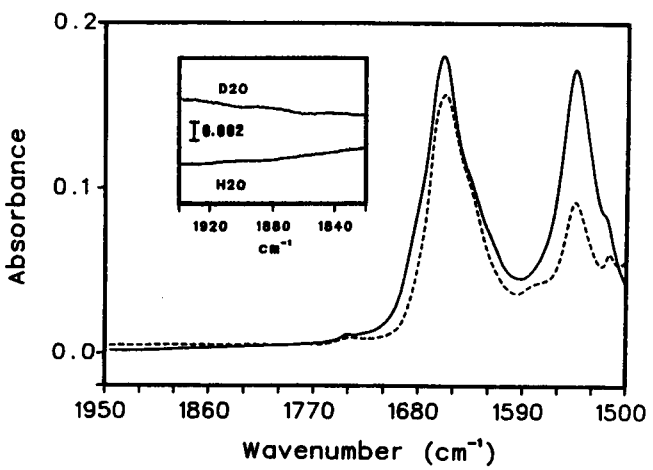

FIGURE 1 Absorption spectra of bleached membrane suspensions in H_2O (——) and in D_2O (– – –), at an instrumental resolution of 1 cm^{-1}. (*Inset*) The region above 1800 cm^{-1} expanded, to show the noise. The bar corresponds to 0.002 AU. Absorption spectra were obtained by coadding 1000 scans in blocks of 20 (20 sample scans and 20 reference scans) of the shuttle accessory, to minimize the water vapor bands.

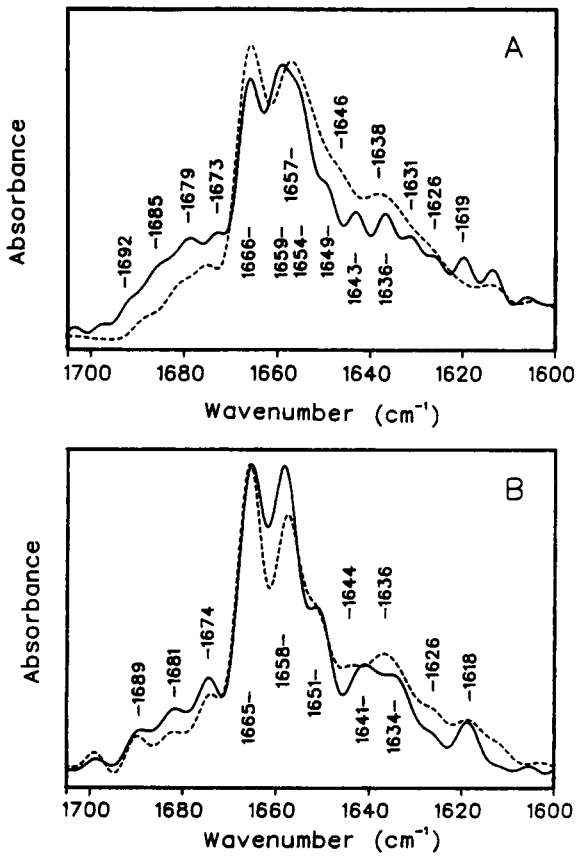

FIGURE 3 (*A*) Deconvoluted spectra of bleached membrane suspensions in H_2O (——) and in D_2O (– – –). (*B*) Deconvoluted spectra of purple membrane suspensions, taken from Cladera et al. (1992b), in H_2O (——) and in D_2O (– – –). The spectra were normalized with respect to the area.

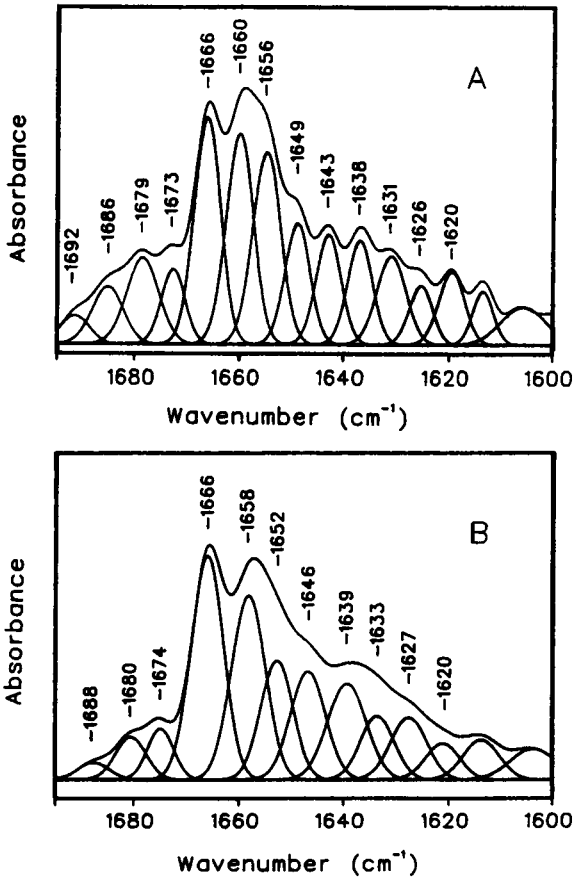

FIGURE 4 Deconvoluted spectra of bleached membrane suspensions with the best-fitted individual component bands. (*A*) In H_2O; (*B*) in D_2O.

4. Some bands that do not correspond to the amide I were included in the curve fitting to avoid the need for a baseline correction.

Table 1 gives the mean relative areas calculated from four independent samples along with the secondary structure assignments. (As a control, we performed the secondary structure quantification of the regenerated purple membrane in H_2O (four independent samples, obtained by incubating the bleached membrane with all-*trans* retinal). The curve-fitted bands were present at the same frequencies as those of native BR, and very similar percentages were obtained for the secondary structures. This indicates that the bleaching treatment does not affect the protein secondary structure.) The two main bands appear at 1666 and 1660 cm^{-1} in H_2O, and at 1666 and 1658 cm^{-1} in D_2O. As for BR (Cladera et al., 1992b), these bands were assigned to the sum of α_{II} and α_I helices (Krim and Dwivedi, 1982), whereas the band at 1656 cm^{-1} was assigned totally to α_I helix (Byler and Susi, 1986; Surewicz and Mantsch, 1988). The band at 1649 cm^{-1} in H_2O was assigned to unordered structure (Byler and Susi, 1986; Surewicz and Mantsch, 1988; Dong et al., 1990). This band probably shifts to 1646 cm^{-1} in D_2O. In our previous work, the band at 1643 cm^{-1} in H_2O was assigned to type III β turns, which correspond to one turn of 3_{10} helix (Krim and Bandekar, 1986; Kennedy et al., 1991). In the spectrum of BO in H_2O we also detected a band at 1643 cm^{-1} in H_2O that, as in the case of BR, seems to shift to 1639 cm^{-1} after incubation in D_2O. Thus, we assigned this band to 3_{10} turns, and this structural type was included in the overall helicoidal structure (i.e., α_I and α_{II} helices plus 3_{10} turns).

In H_2O, the bands between 1620 and 1638 cm^{-1} were assigned to β structure (Byler and Susi, 1986; Surewicz and Mantsch, 1988). In D_2O, a wide feature centered at about 1637–1638 cm^{-1} appears in the deconvoluted spectrum, which corresponds to the sum of the 1639 and 1633 cm^{-1} curve-fitted bands (Fig. 4 *B*). These bands probably originate from the shift of those absorbing at 1643 cm^{-1} (as mentioned above) and 1638 cm^{-1} in H_2O, respectively.

The bands observed in the region between 1673 and 1690 cm^{-1} were assigned to reverse turns in both H_2O and D_2O, and from comparison of the deconvoluted spectra displayed in Fig. 3, a shift of part of these structures to frequencies below 1670 cm^{-1} upon deuteration can be deduced. In fact, it is clear that the value corresponding to reverse turns in D_2O is lower than for the sample in H_2O and that the content in helical structure is higher (Table 2). These dif-

TABLE 1 Position, fractional areas, and assignments of the amide I bands of bleached membrane

H_2O			D_2O		
Freq.*	% area#	Assignment	Freq.*	% area#	Assignment
1686	3.9 ± 0.8	Reverse turns	1688	1.2 ± 0.2	Reverse turns
1679	6.8 ± 1.6	Reverse turns	1680	4.8 ± 0.7	Reverse turns
1673	5.3 ± 1.5	Reverse turns	1674	3.4 ± 0.6	Reverse turns
1666	17.6 ± 1.1	α_{II} helix	1666	20.2 ± 1.0	α_{II} helix + turns
1660	12.7 ± 1.5	α_{II} + α_{I} helix	1658	20.8 ± 1.4	α_{II} + α_{I} helix
1656	16.1 ± 1.3	α_{I} helix	1652	10.8 ± 1.1	α_{I} helix
1649	8.9 ± 0.3	Unordered	1646	11.7 ± 1.2	Unordered
1643	7.2 ± 0.3	3_{10} turns	1639	9.6 ± 0.6	3_{10} turns
1638	6.7 ± 1.3	β	1633	6.5 ± 1.0	β
1632	5.8 ± 1.6	β	1627	5.2 ± 3.2	β
1627	4.7 ± 0.1	β	1620	5.6 ± 2.6	β
1620	4.3 ± 1.0	β			

* Frequency positions are expressed in cm^{-1}, and are rounded off to the nearest integer.
# Mean relative areas calculated from 4 independent experiments. The standard deviation is also indicated.

ferences can be explained assuming that, after H/D exchange, part of the bands in the reverse turns region shift to the α-helical region.

Quantification of the secondary structure of proteins from curve-fitted bands on the deconvoluted spectrum may introduce some potentially significant errors arising from the mathematical treatment (for a recent review see Jackson and Mantsch, 1995). The Fourier self-deconvolution function operates with a single bandwidth on the IR spectrum, which is formed by individual components, the bandwidths of which would probably be different. This fact may produce band distortions, which after curve fitting may lead to over- or underestimation of the considered band areas. In a previous paper on the secondary structure of BR, we described a procedure for taking into account these distortions (Cladera et al., 1992b). The synthetic spectrum used for determining the best parameters of deconvolution (see Fig. 2 of the present paper) was deconvoluted and curve fitted, and the resulting bands were compared with the known component bands of the synthetic spectra. This allowed us to estimate the errors introduced by the deconvolution treatment (i.e., the methodological errors). We assume that the errors will be very similar for the curve fitting of the experimental deconvoluted spectra. Following this procedure, we estimated the methodological errors in the BO secondary structure quantification and we added them to the experimental errors. The secondary structure of BO in H_2O can be summarized as follows (Table 2): 53.7 ± 7.7% helicoidal structure (α_{I} and α_{II} helix plus 3_{10} turns), 15.9 ± 2.9% reverse turns, 21.4 ± 2.8% β structure, and 8.9 ± 3.8% unordered structure. These values can be compared to those of BR (Cladera et al., 1992b): 62.5 ± 10.5% α-helices, 16.0 ± 3.0% reverse turns, 13.5 ± 2.5% β structure, and 5.0 ± 2.0% unordered segments. Therefore, after retinal removal the structural types of native BR are still present in the apoprotein: 3_{10} turns and α_{II} helix are present (the latter slightly decreased), and the helicoidal structures remain the predominant structural type.

We have not succeeded in calculating exactly the differences in H/D exchange between BO and BR from the amide II/amide I intensity ratios before and after deuteration. The accurate determination of these intensities was greatly influenced by difficulties in locating the baseline, and by the presence of intense bands near the amide II region. Nevertheless, our estimations indicate that H/D exchange in BO samples is 15–20% higher than in BR. In particular, the

TABLE 2 Percentage composition of secondary structure of bleached membrane as compared to the purple membrane*

BO				BR#			
H_2O		D_2O		H_2O		D_2O	
Structure	Area (%)	Structure	Area (%)	Structure	Area (%)	Structure	Area (%)
Reverse turns	15.9 ± 2.9	Reverse turns	9.4 ± 1.2	Reverse turns	15.8 ± 2.6	Reverse turns	13.4 ± 1.8
Helix§	53.7 ± 7.7	Helix§ + turns	61.4 ± 7.1	Helix§ + unordered	66.2 ± 8.3	Helix§ + turns	65.4 ± 14.4
β	21.4 ± 2.8	β	17.3 ± 2.2	β	17.2 ± 2.7	β	15.1 ± 8.0
Unordered	8.9 ± 3.8	Unordered	11.7 ± 5.9	Unordered	—¶	Unordered	4.9 ± 2.4

* The experimental error was obtained as follows: 1) Spectra corresponding to four independent samples were used in each case. For each sample, the band areas assigned to a same structure were added up and averaged with the values obtained for the other samples. 2) The standard deviation for each structure was calculated from the values obtained for the four samples.
# Taken from Cladera et al. (1992b).
§ α_{I} and α_{II} helices plus 3_{10} turns.
¶ For purple membrane in H_2O, the unordered structure content cannot be separated from that of total helix content. Only after D_2O incubation can this structure be estimated (see Cladera et al., 1992b).

comparison of the degree of H/D exchange for the loops region (bands between 1673 and 1690 cm^{-1}) for BO and BR shows a clear increase for the former (about 41% for BO and 15% for BR). This argues in favor of a more open conformation of the loops in the apomembrane, and suggests that the retinal molecule is able to elicit detectable changes in the external loops by altering the compactness of the transmembrane helices. This is in keeping with the well-known fact that the B-C loop is readily accessible to α-chymotrypsin in the apomembrane, but only to a limited extent in the native BR (Gerber et al., 1977). On the other hand, Fig. 5 shows that the acidic residues are also more exposed to the solvent in the apomembrane. Both BR and BO in H_2O (Fig. 5 *A*) show a peak centered at 1741 cm^{-1} corresponding to acidic amino acid absorptions (Chirgadze et al., 1975; Braiman et al., 1988; Sasaki et al., 1994). After deuteration, part of this band shifts to 1729 cm^{-1} in BR, whereas in the case of BO the band at 1741 cm^{-1} shifts completely to 1729 cm^{-1} (Fig. 5 *B*). This is compatible with the presence in BR of carboxylic groups buried in the membrane, which upon bleaching become accessible to the medium.

The results presented in this work show that the native secondary structure is essentially defined in the apoprotein (BO), and the retinal removal does not dramatically affect the secondary structure quantitative distribution. This is in agreement with the results presented by London and Khorana (1982) in their study about denaturation and renaturation of bacteriorhodopsin in artificial media (detergents and lipid-detergent mixtures). Using circular dichroism, these authors pointed out that native-like secondary structure spontaneously reforms upon the addition of phospholipid/cholate mixtures to bacterioopsin denatured in sodium dodecyl sulfate. However, as our deuterium exchange experiments indicate, retinal removal has an effect on both the protein tertiary structure and the loops.

Popot and Engelman (1990) proposed that the folding of an integral membrane protein could be described by a two-step process: 1) the formation of independent helicoidal segments in the bilayer, and 2) the interaction of the helices to form functional tertiary structures. The results give further support to the idea of the retinal molecule as a compacting element in BR, with a structural contribution that is more important for the definition of interhelical interactions than for secondary structure formation. Thus, retinal appears to be an important element in the BR folding process, being crucial in defining the native interhelical interactions, which represents the second step. This view is further supported by several previous results. For example, BO in H_2O does not present any appreciable calorimetric transition, but at the same time shows secondary structural changes very similar to those of BR upon thermal denaturation (Cladera et al., 1992a). This was interpreted as a noncooperative denaturation behavior directly related to a looser disposition of the BO polypeptide in the membrane, resulting from weaker interhelical interactions. A more open conformation of the protein structure on bleaching has previously been suggested on the basis of spectroscopic studies (Becher and Cassim, 1977; Acuña et al., 1984).

The influence of the retinal molecule on the conformation and accessibility of the loops, as described in our work, can be related to the reported movement of some helices occurring in the M intermediate of the BR photocycle (Subramaniam et al., 1993). In this later case, deprotonation of the Schiff base is likely to decrease or even cancel the network of ionic and hydrogen bonding interactions involving the protonated Schiff base. This can give rise to a similar effect as removing retinal, although less intense.

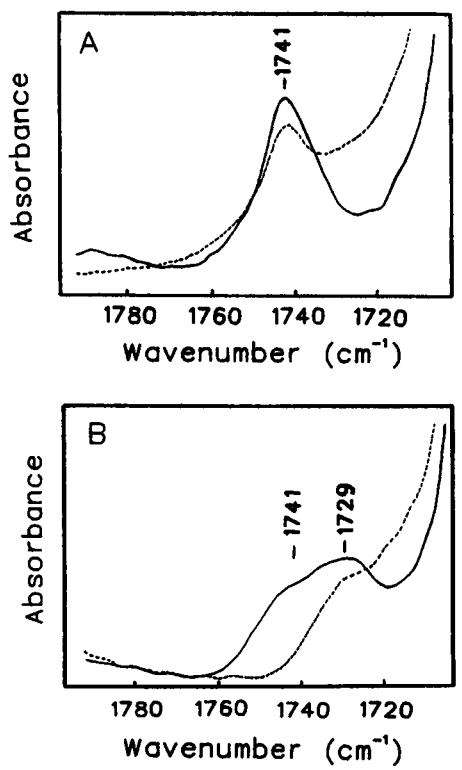

FIGURE 5 Absorption spectra correspoding to the protonated carboxylic lateral chains of purple membrane suspensions (——) and bleached membrane suspensions (– – –). (*A*) In H_2O; (*B*) in D_2O.

The excellent technical assistance of Elodia Serrano and Daniel Peris is gratefully acknowledged. This work was supported by grant PB92-0622 from the Dirección General de Investigación Científica y Técnica, and grant GRQ93-2026 from the Direcció General de Recerca.

REFERENCES

Acuña, A. V., J. González, M. P. Lillo, and J. M. Otón. 1984. The UV protein fluorescence of purple membrane and its apomembrane. *Photochem. Photobiol.* 40:351–359.

Becher, B., and J. Y. Cassim. 1977. Effects of bleaching and regeneration on the purple membrane structure of *Halobacterium Halobium*. *Biophys. J.* 19:285–297.

Braiman, M. S., T. Mogi, T. Marti, L. Stern, H. G. Khorana, and K. J. Rothschild. 1988. Vibrational spectroscopy of bacteriorhodopsin mutants: light-driven proton transport involves protonation changes of aspartic acid residues 85, 96, and 212. *Biochemistry.* 27:8516–8520.

Burghaus, P. A., and N. A. Dencher. 1989. The chromophore retinal hinders passive proton-hydroxide ion translocation through bacteriorhodopsin. *Arch. Biochem. Biophys.* 275:395–409.

Byler, D. M., and H. Susi. 1986. Examination of the secondary structure of proteins by deconvolved FTIR spectra. *Biopolymers.* 25:469–487.

Chirgadze, Y. N., O. V. Fedorov, and N. P. Trushina. 1975. Estimation of amino acid residue side-chain absorption in the infrared spectra of protein solutions in heavy water. *Biopolymers.* 14:679–694.

Cladera, J., M. L. Galisteo, M. Sabés, P. L. Mateo, and E. Padrós. 1992a. The role of retinal in the thermal stability of the purple membrane. *Eur. J. Biochem.* 207:581–585.

Cladera, J., M. Sabés, and E. Padrós. 1992b. Fourier transform infrared analysis of bacteriorhodopsin secondary structure. *Biochemistry.* 31: 12363–12368.

Dong, A., P. Huang, and W. S. Caughey. 1990. Protein secondary structures in water from second-derivate amide I infrared spectra. *Biochemistry.* 29:3303–3308.

Duñach, M., E. Padrós, A. Muga, and J. L. Arrondo. 1989. Fourier-transform infrared studies on cation binding to native and modifield purple membranes. *Biochemistry.* 28:8940–8945.

Duñach, M., M. Seigneuret, J.-L. Rigaud, and E. Padrós. 1986. The relationship between the chromophore moiety and the cation binding sites in bacteriorhodopsin. *Biosci. Rep.* 6:961–966.

Ebrey, T. 1993. Light energy transduction in bacteriorhodopsin. *In* Thermodinamics of Membranes, Receptors and Channels. M. Jackson, editor. CRC Press, Boca Raton, FL. 353–387.

Gerber, G. E., C. P. Gray, D. Wildenauer, and H. G. Khorana. 1977. Orientation of bacteriorhodopsin in *Halobacterium halobium* as studied by selective proteolysis. *Proc. Natl. Acad. Sci. USA.* 74:5426–5430.

Henderson, R., J. M. Baldwin, T. A. Ceska, F. Zemlin, E. Beckmann, and K. H. Downing. 1990. Model for the structure of bacteriorhodopsin based on high-resolution electron cryo-microscopy. *J. Mol. Biol.* 213: 899–929.

Jackson, M., and H. H. Mantsch. 1995. The use and misuse of FTIR spectroscopy in the determination of protein structure. *Crit. Rev. Biochem. Mol. Biol.* 30:95–120.

Kennedy, D. F., M. Crisma, C. Toniolo, and D. Chapman. 1991. Studies of peptides forming 3_{10}- and α-helices and β-bend ribbon structures in organic solution and in model biomembranes by Fourier transform infrared spectroscopy. *Biochemistry.* 30:6541–6548.

Khorana, H. G. 1988. Bacteriorhodopsin, a membrane protein that uses light to translocate protons. *J. Biol. Chem.* 263:7439–7442.

Krimm, S., and J. Bandekar. 1986. Vibrational spectroscopy and conformation of peptides, polypeptides, proteins. *Adv. Protein Chem.* 38: 181–364.

Krimm, S., and A. M. Dwivedi. 1982. Infrared spectrum of the purple membrane: clue to a proton conduction mechanism? *Science.* 216: 407–408.

Lanyi, J. K. 1993. Proton translocation mechanism and energetics in the light-driven pump bacteriorhodopsin. *Biochim. Biophys. Acta.* 1183: 241–261.

London, E., and H. G. Khorana. 1982. Denaturation and renaturation of bacteriorhodopsin in detergents and lipid-detergent mixtures. *J. Biol. Chem.* 257:7003–7011.

Mantsch, H. H., D. J. Moffatt, and H. Casal. 1988. Fourier transform methods for spectral resolution enhancement. *J. Mol. Struct.* 173: 285–298.

Moffatt, D. J., J. K. Kauppinen, D. G. Cameron, H. H. Mantsch, and R. N. Jones. 1986. Computer Programs for Infrared Spectrophotometry, NRCC Bulletin 18. National Research Council of Canada, Ottawa, Canada.

Oesterhelt, D., L. Schuhmann, and H. Gruber. 1974. Light-dependent reaction of bacteriorhodopsin with hydroxylamine in cell suspensions of *Halobacteirum halobium*: demonstration of an apo-membrane. *FEBS Lett.* 44:257–261.

Oesterhelt, D., and W. Stoeckenius. 1973. Functions of a new photoreceptor membrane. *Proc. Natl. Acad. Sci. USA.* 70:2853–2857.

Oesterhelt, D., and W. Stoeckenius. 1974. Isolation of the cell membrane of *Halobacterium halobium* and its fractionation into red and purple membrane. *Methods Enzymol.* 31:667–678.

Popot, J. L., and D. M. Engelman. 1990. Membrane protein folding and oligomerization: the two-stage model. *Biochemistry.* 29:4031–4037.

Rothschild, K. 1992. FTIR difference spectroscopy of bacteriorhodopsin: toward a molecular model. *J. Bioenerg. Biomembr.* 24:147–167.

Sasaki, J., J. K. Lanyi, R. Needleman, T. Yoshizawa, and A. Maeda. 1994. Complete identification of C=O stretching vibrational bands of protonated aspartic acid residues in the difference infrared spectra of M and N intermediates versus bacteriorhodopsin. *Biochemistry.* 33:3178–3184.

Stoeckenius, W., and R. Bogomolni. 1982. Bacteriorhodopsin and related pigments of halobacteria. *Annu. Rev. Biochem.* 52:587–616.

Subramaniam, S., M. Gerstein, D. Oesterhelt, and R. Henderson. 1993. Electron diffraction analysis of structural changes in the photocycle of bacteriorhodopsin. *EMBO J.* 12:1–8.

Surewicz, W. K., and H. H. Mantsch. 1988. New insight into protein secondary structure from resolution-enhanced infrared spectra. *Biochim. Biophys. Acta.* 952:115–130.

Vogel, H., and W. Gärtner. 1987. The secondary structure of bacteriorhodopsin determined by raman and circular dichroism spectroscopy. *J. Biol. Chem.* 262:11464–11469.